Atmos. Chem. Phys. Discuss., https://doi.org/10.5194/acp-2018-128
Manuscript under review for journal Atmos. Chem. Phys.
Discussion started: 16 February 2018

Atmospheric Chemistry and Physics Discussions

Impact of tropical lower stratospheric cooling on deep convective activity: (I) Recent trends in tropical circulation

Kunihiko Kodera[1], Nawo Eguchi[2], Rei Ueyama[3, 4], Yuhji Kuroda[5], and Chiaki Kobayashi[5]
[1] Institute for Space-Earth Environmental Research, Nagoya University, Nagoya, 464-8601, Japan
[2] Research Institute for Applied Mechanics, Kyushu University, Kasuga, 816-8580, Japan
[3] NASA Ames Research Center, Moffett Field, 94035-0001, USA
[4] Bay Area Environmental Research Institute, Moffett Field, 94035-0001, USA
[5] Meteorological Research Institute, Tsukuba, 305-0052, Japan

Correspondence to: Kunihiko Kodera (f)

Abstract. Large changes in tropical circulation, in particular those related to the summer monsoon and cooling of the sea surface in the equatorial eastern Pacific, were noted from the mid to late 1990s. The cause of such recent decadal variations in the tropics was studied by making use of a meteorological reanalysis dataset. Cooling of the equatorial southeastern Pacific Ocean occurred in association with enhanced cross-equatorial southerlies, which resulted from a strengthening and poleward shift of the rising branch of the boreal summer Hadley circulation connected to the stratospheric Brewer–Dobson circulation. From boreal summer to winter, the anomalous convective activity centre moves southward following the seasonal march to the equatorial Indian Ocean–Maritime Continent region, which strengthens the surface easterlies over the equatorial central Pacific. Accordingly, ocean surface cooling extends over the equatorial central Pacific. We suggest that the fundamental factor causing the recent decadal change in the tropical troposphere and the ocean is a poleward shift of the rising branch of the summertime Hadley cell, which can result from a strengthening of extreme deep convection penetrating into the tropical tropopause layer, in particular over the continents of Africa and Asia, and adjacent oceans. We conjecture that this effect is produced by a combination of land surface warming due to increased CO_2 and a reduction of static stability in the tropical tropopause layer due to tropical stratospheric cooling.

1 Introduction

Large changes in tropical circulation occurred from the mid to late 1990s. These include a slowdown, or hiatus, of global warming in association with a decrease in the tropical eastern Pacific sea surface temperature (SST) (Kosaka and Xie, 2013; England et al., 2014; Trenberth et al., 2014; Watanabe et al., 2014). Changes were also found in the advancement of the onset of the Asian summer monsoon (Kajikawa et al., 2012; Gautam and Regmi, 2013; Xiang and Wang, 2013; Yun et al., 2014) and an increase in precipitation in West Africa over the Sahel (Fontaine et al., 2011; Brandt et al., 2014; Maidment et al., 2015, Diawara et al., 2016). An increase in precipitation in southern Africa was also noted during the austral summer (Vizy and Cook, 2016). Besides these large-scale circulation changes, changes in mesoscale phenomena such as an increase in the cyclone frequency and intensity over the Arabian Sea were also reported (Evan and Camargo, 2011). Wang et al.

(2012) pointed out that these phenomena are, in fact, related to the abovementioned early onset of the Asian summer monsoon. A relationship between tropopause layer cooling and tropical cyclone activity in the Atlantic has also been suggested (Emanuel et al., 2013). Indeed, recent numerical model studies show that cooling of the tropopause impacts the intensity of tropical storms as well as SSTs (Ramsay, 2013; Wang et al., 2014). In this respect, the recent cooling of the tropical tropopause and lower stratosphere from around 2000 (Randel et al., 2006; Randel and Jensen, 2013) should be investigated together with tropical tropospheric change.

The importance of the Pacific Decadal Oscillation (PDO) on decadal changes in global temperature and precipitation has been noted (Meehl et al., 2013; Dong and Dai, 2015; Trenberth, 2015). The most recent hiatus ended around 2013 followed by a large warming due to an El Niño event in 2015 (Hu and Fedorov, 2017; Liu and Zhou, 2017; Urabe et al., 2017; Xie and Kosaka, 2017). However, the El Niño of 2015/16 was different from the previous large 1997/98 El Niño with less warming in the eastern Pacific (Paek et al., 2017), conforming to an increasing trend of the central Pacific-type El Niño (Kao and Yu, 2009; Johnson, 2013). In this sense, the anomalous tropical circulation from the 1990s did not terminate with the hiatus, but is persisting. Similarly, the northward shift of the convective zone in the boreal summer still continues, as shown below.

As a cause of recent tropical changes, multidecadal variations of the atmosphere–ocean coupled mode such as the Atlantic Multidecadal Oscillation have also been proposed (Wang et al., 2013; Kamae et al., 2017). The possible impact of SSTs in different oceanic basins on recent trends in monsoon precipitation was studied by using a coupled ocean model by Kamae et al. (2017). Their results show that the change in Atlantic SST can reproduce recent increasing trends in monsoon rainfall in the northern hemisphere (NH), except for the Asian monsoon. The Atlantic SSTs, however, have practically no effect on the southern hemisphere (SH) such as the African and Australian monsoons. Another difference from observations is that the simulated increase in rainfall occurs mainly over the oceans in low latitudes between the equator and 15° N rather than over continents between around 10° N and 20° N as observed (see Fig. 3 of Kamae et al., 2017). Thus, it is difficult to attribute the recent global trends to a regional mode of decadal oceanic variation alone. In this paper, we first show that the fundamental factor causing the recent decadal trend in the tropics from the mid to late 1990s is not the PDO, but rather a poleward shift of the summertime rising branch of the Hadley circulation connected to the upwelling branch of the stratospheric Brewer–Dobson circulation.

One aspect of the recent trends in tropical circulation that has been reported is the poleward expansion of the tropics (e.g., Davis and Rosenlof, 2012). The expansion of the tropics is rather related to a change in the sinking branch of the Hadley cell driven by midlatitude transient eddies (Kang and Polvani, 2011). There are also other phenomena showing large trends in high latitudes and polar regions that are a part of global change and could be related to tropical change. However, in the interest of brevity, this paper focuses on changes in the tropics.

The paper is organized as follows. After describing the data used for the study in Sect. 2, the results of our analysis are presented in Sect. 3. Finally, a summary and discussion of the causes of the recent tropical changes are presented in Sect. 4.

2 Data

We make use of meteorological reanalysis data produced by the Japan Meteorological Agency (JMA), JRA55 (Kobayashi et al., 2015). A large discontinuity was found at the end of the 1990s in the previous reanalysis product, JRA25, when the TIROS Operational Vertical Sounder (TOVS) on board the National Oceanic and Atmospheric Administration (NOAA) satellite was switched to Advanced TOVS (ATOVS) (Li et al., 2000). This discontinuity has largely been reduced in the JRA55 reanalysis (Kobayashi et al., 2015). To investigate deficiencies in the general circulation model, we make use of a family of JRA55 product: AMIP-type Simulation (JRA55-AMIP), which uses the same model and boundary conditions as JRA55 reanalysis, but without assimilation of observational data in the atmosphere.

Outgoing longwave radiation (OLR) data provided by NOAA are widely used for analysis of convective activity in the tropics. In the present study, we use monthly mean OLR data (1° × 1° latitude–longitude resolution) derived from the High Resolution Infrared Radiation Sounder (HIRS) (Lee et al., 2007), available at ftp://eclipse.ncdc.noaa.gov/cdr/hirs-olr/monthly/. Analysis of the precipitation is performed by making use of Global Precipitation Climatology Project (GPCP) monthly mean data Ver.2.3 (Adler et al., 2003). COBE monthly mean gridded SST data with 1° × 1° boxes compiled by the JMA (Ishii et al., 2005) are used for the study of oceanic surface change.

Climatology is defined by the 30-year mean from 1981 to 2010 in the present study. Seven El Niño events after 1979 are defined by the JMA based on 6-monthly mean SSTs in the Niño 3 sector (5° S–5° N, 150° W–90° W) (available at http://ds.data.jma.go.jp/gmd/tcc/tcc/products/elnino/ensoevents.html). In this study, we define the NH cold seasons 1982/83, 1986/87, 1991/92, 1997/98, 2002/03, 2009/10, and 2015/16 as El Niño winters.

3 Results

3.1 Eastern Pacific cooling

The recent poleward shift of the convergence zone in the boreal summer is identified from the July–September mean anomalous OLR in 1999–2016 from 30-year climatology (1981–2010) (Fig. 1a). A northward shift of the convective activity is seen around the summer monsoon regions over Africa, Asia, and Central America. A poleward shift is further evident in the zonal-mean OLR in Fig. 1b. Climatological OLR peaks around 10° N, while anomalous OLR of the recent period has a maximum around 15° N.

There is a close relationship between the position of the tropical convergence zone and the development of cold tongues in the tropical oceans. Figure 2 shows the climatological mean annual cycle in zonal mean OLR, meridional wind at 925 hPa, and equatorial SSTs in the eastern Pacific−Atlantic sector. When convective activity, identified by low values of the OLR, shifts northward during boreal summer, cross-equatorial southerlies become stronger west of the American and African continents, which lead to a decrease in the SSTs along the coastal regions. Thus, the primary factor producing cold tongues in the tropical SSTs is the shape of continents, air–sea interaction, and the position of the rising branch of the Hadley circulation, as described in Xie and Philander (1994) and Xie (2004). Therefore, changes in the rising branch of the Hadley circulation, such as can be seen in Fig. 1, can directly impact the equatorial eastern Pacific SSTs.

To investigate whether the northward shift of the convective zone is driven by the PDO, anomalous OLR during the two periods of neutral and negative phases of the PDO is displayed in Figs. 1c and 1d together with anomalous SSTs during those time periods (Figs. 1e and 1f). A characteristic horseshoe pattern in the north Pacific SST is evident during the negative phase of the PDO. Anomalous OLR indicates that the convective activity is enhanced along 15° N–20° N latitude irrespective of the phase of the PDO, except for the sector under the direct influence of the PDO in the eastern Pacific, where cooling is larger during the negative phase. However, even during the neutral phase of the PDO, negative anomalies in the SST exist in the tropics west of South America. This suggests that the SST cooling west of South America is not solely driven by the PDO, but is related to the strengthening and northward shift of the convergence zone.

The seasonal dependence of the recent trend in tropical convective activity is depicted in Fig. 3. The panels on the left show latitude–time sections of 3-monthly mean anomalous zonal-mean OLR from 1979 to 2016. To better illustrate the evolution in latitudinal structure, the tropical mean (10° S–25° N) is further subtracted from the temporal anomaly in Fig. 3a. Inspection reveals a change in zonal-mean OLR around 1999 (vertical lines) in all four seasons: the convergence zone in the NH tends to be located at higher latitudes in recent years compared to the previous period. The anomalous negative zone shifts northward after 1999 from boreal spring to summer and descends to lower latitudes from boreal summer to autumn following the seasonal march.

The horizontal structure of the anomalous OLR in the recent period (1999–2016) is depicted in the panels on the right for each season: April, May and June (AMJ), July, August and September (JAS), October November and December (OND), and January, February, and March (JFM). The anomalous negative centre of OLR is located around the Maritime Continent during boreal spring, which shifts northward by spreading longitudinally along 15° N, in particular along the African and Asian sectors during boreal summer. Next, the negative OLR region shifts and clusters over the Indian Ocean region during boreal autumn. At the same time, positive OLR anomalies develop over the equatorial eastern Pacific, suggesting a suppression of convective activity over the Pacific Ocean. During boreal winter, the anomalous convective active region

shifts eastward over the Maritime Continent, and suppression of convective activity over the eastern Pacific is sustained during the cold season.

The impact of the recent decadal variation of convective activity on the SST is depicted in Fig. 4. The top panels show the 1999–2016 mean anomalous OLR in (a) JAS, (b) OND. The anomalous horizontal winds at 925 hPa and SSTs are presented in the bottom panels. Because the response of the SST arises following atmospheric circulation, anomalous SSTs during the following month (i.e., August, September and October (ASO) and November, December and January (NDJ)) are displayed in Figs. 4c and 4d, respectively. In JAS, the anomalous cross-equatorial flow west of South America intensifies due to a poleward shift of a rising branch of the Hadley cell. The cross-equatorial flow changes from westward to eastward when it crosses the equator. This results in a strengthening of the climatological easterlies in the SH and enhances anomalous convergence near New Guinea. In contrast, easterlies are weakened in the NH, which explains a warming in the north, but a cooling south of the equator. Such a meridional seesaw of the anomalous SSTs and cross-equatorial flow suggests an important role for wind−evaporation−SST (WES) feedback (Xie and Philander, 1994) in recent trends. The centre of anomalous negative OLR moves to the equatorial eastern Indian Ocean from boreal summer to autumn, which results in a strengthening of anomalous easterlies over the equatorial central Pacific and a westward extension of low SSTs over the equator.

The impact of cooling of the eastern equatorial Pacific in the SH can also be seen as a structural change in El Niño/Southern Oscillation (ENSO) phenomena after 1999. Figure 5 shows a longitude–time section of the anomalous OLR over the equatorial SH (0°–10° S). Convective activity largely increases over the Pacific during El Niño events before 1999. However, after 1999, Pacific convective activity is suppressed; an increase in convective activity during El Niño is apparent only over the central Pacific. In contrast, convective activity west of 160° E over the Maritime Continent generally increases after 1999.

3.2 Vertical structure

A northward shift of convective activity is observed during boreal summer. Normally, Asian summer monsoons start from the pre-Meiyu season around 27 May, and the convective activity jumps northward in midsummer around 18 July (Chiang et al., 2017). Differences in the northward shift of the convection between the recent decadal period (1999–2016 mean JAS anomalies) and the climatological seasonal march around the onset of midsummer (18 July) are depicted in Fig. 6. The horizontal structure of the OLR related to the recent trend (Fig. 6a) is similar to that related to the change around the onset of midsummer (Fig. 6b): On one hand, this pattern is characterized by increased convection around 15° N, in particular over Africa and Asia and the western Pacific; on the other hand, convective activity over the equatorial region is generally suppressed, except for New Guinea in recent trends. The bottom panels compare meridional sections of zonal mean pressure vertical velocity during the same time periods as the top panels. Climatological mean pressure vertical velocity is also

indicated by contours. In spite of the similarity of the horizontal structure of the OLR, the vertical structure of the pressure vertical velocity is largely different. In the case of the seasonal march (Fig. 6d), changes occur mainly horizontally as northward in the tropospheric. A northward shift in the recent trend in the lower troposphere is more or less similar to that in seasonal march (Fig. 6c). However, the vertical structure is quite different: In the upper troposphere, upwelling extends vertically to the tropical tropopause layer (TTL) along the rising branch of Hadley circulation indicated by climatological upwelling region (contours in Fig. 6c). In the equatorial SH, intensification of upwelling is observed in the troposphere, but this does not extend into the stratosphere.

The recent increasing trend in the tropical lower stratospheric upwelling at 70 hPa, together with the increasing number of sudden stratospheric warming events, was identified by Abalos et al. (2015). It has been suggested that increased stratospheric tropical upwelling tends to enhance deep convective activity, in particular deep penetrating clouds, through change in the static stability of the TTL (Eguchi et al., 2015; Kodera et al., 2015). A height–time section of the zonal mean temperature around the tropopause, together with the zonally averaged pressure vertical velocity at 70 hPa, shows year-to-year variation of the temperature associated with the quasi-biennial oscillation superimposed on a decadal cooling trend in the lower stratosphere. In the upper troposphere, warming pulses related to El Niño events are superimposed on a warming trend in the troposphere (Fig. 7). A decrease in lower stratospheric temperature and an increase of upper tropospheric temperature lead to a decrease in the static stability of the TTL.

To investigate the coupling between the stratospheric and tropospheric variations in the tropics, a singular value decomposition (SVD) analysis (Kuroda, 1998) was conducted. First, we performed SVD analysis on the zonal mean pressure vertical velocity around the TTL (30° S–30° N, 300–70 hPa) and the horizontal distribution of the OLR in the tropics (30° S–30° N) during boreal summer (JAS) based on the covariance matrix. Each value at the grid point was weighted by the cosine of the latitude and the layer thickness. The results are presented in Fig. 8. The left panels show the time coefficients. The middle and right panels are heterogeneous correlations with OLR and the zonal mean vertical pressure velocity, respectively. To get a general view of the troposphere and stratosphere, the heterogeneous correlation of the vertical velocity is extended to a height range of 1000 to 10 hPa.

The leading SVD mode (Fig. 8a) is related to the ENSO phenomenon. When El Niño occurs, convection over the equatorial central–eastern Pacific becomes active (negative OLR) and the time coefficients become large. Especially large amplitudes are found during the El Niño events of 1997/98 and 2015/16. The three types of El Niño identified by Paek et al. (2017) are indicated above the time coefficients. The time coefficients of the second mode exhibit an increasing trend (Fig. 8b). The variation of the zonal mean pressure vertical velocity of the leading mode is confined essentially in the troposphere below 100 hPa, whereas that of the second mode extends into the lower stratosphere. Note that the upwelling of the second mode is also related to the variation of the middle stratosphere in the SH. This implies a strengthening of the Hadley circulation in

connection with the enhancement of the Brewer–Dobson circulation. Tropospheric anomalous upwelling is disconnected from the stratosphere in the equatorial SH. A horizontal map of the OLR indicates that the upwelling region is located over the Maritime Continent. This increase in the regional convective activity is, in fact, coupled to a suppression of upwelling over surrounding oceans.

In the above analysis, we made use of the covariance matrix to calculate the SVD. In this case, a mode of variability having large amplitude such as the ENSO is extracted as the leading mode. To extract a variation of smaller amplitude but spreading over a large area, the use of normalized covariance, or the correlation matrix, may be appropriate. In such an analysis, the second mode in the previous analysis becomes the leading mode (Fig. 8c). An increasing trend related to the stratospheric circulation and the northward shift of convection over the Asian–African sector becomes further obvious. The ENSO related variation becomes the second mode (Fig. 8d). The spatial structure of the OLR of this mode is slightly modified: negative OLR extends less eastward over the equatorial central Pacific. Accordingly, the time coefficients of the east Pacific type El Niño become smaller compared to those in Fig. 8a, and a slight increasing trend appears in the time series.

To focus on the stratosphere-related variation during the boreal summer, the JAS mean vertical pressure velocity (ω) at 30 hPa averaged over tropical SH (0°–25° S) is chosen as the index of stratospheric mean meridional circulation (I_ω) (Fig. 9a). The correlation coefficient between I_ω and zonal mean ω at each grid point (Fig. 9b) shows a correlation pattern very similar to the leading mode in Fig. 8c. To indicate the relationship between the climatological residual mean-meridional circulation, the mass-weighted stream function diagnosed by the method of Iwasaki (1992) is displayed by contours in Figs. 9b and 9c. We can see that the variation in stratospheric upwelling in the Brewer–Dobson circulation is connected to the Hadley circulation in the TTL around 15° N.

The same correlation, but with the zonal-mean temperature at each grid point from the 90°S to 90°N, is shown in Fig. 9c. The tropical upwelling is not only related to a cooling in the tropics and the summer hemisphere, but it is also related to a warming in the downwelling region around the winter polar stratosphere (Fig. 9c). This illustrates the dynamical nature of the recent tropical stratospheric cooling. Stratospheric upwelling is also connected with convective activity along 15° N−20° N (Fig. 9d), as already discussed above. The correlation coefficients between I_ω and 925 hPa zonal and meridional winds at each grid point are shown by arrows in Fig. 9e. An increase in the cross-equatorial winds in the eastern Pacific and Atlantic is observed. The impact of near surface wind variation on the SST can be seen in the lagged correlation with the SST in Fig. 9e. The cooling in the equatorial eastern Pacific is largest with a time lag of 5 months (i.e., December, January and February (DJF)), consistent with the development of La Niña–like SSTs from boreal autumn in Fig. 4.

Here we have simply shown possible relationships among the variables. However, a discussion of the statistical significance of the relationships between variables that exhibit large trends in a short data record is practically impossible. Thus, we will address this issue in a companion paper focusing on transient events (Kodera et al., in preparation).

3.3 Convection over continents and ocean

Two different modes of variability extracted by the SVD analysis in Fig. 8 are particularly pronounced, one over continents and the other over ocean sectors. Here we examine the characteristics of the variations in two sectors: the African continent (10° W–40° E) and the Pacific Ocean (170° W–120° W). The Pacific sector corresponds to the longitudes of Niño 3.4. To identify the different characteristics of convective activity over continents and ocean, the climatological annual cycle in the zonal mean pressure vertical velocity at 300 hPa is depicted in Figs. 10a and 10d. A region of enhanced convective activity migrates north and south over the continent following the seasonal variation of solar heating. It should be noted that the convective zone over Africa shows a jump during the summer monsoon season (Hagos and Cook, 2007). In the case of the Pacific Ocean, the convective zone shows only a small latitudinal excursion and is located in the NH around 5° N throughout the year.

Latitude–time sections of the 3-monthly mean anomalous (departures from climatology) 300 hPa pressure vertical velocity are shown in Figs. 10b and 10e from February 1979 to November 2016. Over the African sector (Fig. 10b), the vertical velocity increases from the mid-1990s in both hemispheres around 10°−20° in latitude corresponding to the rising branch of the summertime Hadley circulation in the TTL. Accordingly, the annual mean precipitation over Africa increases in the recent period (1999−2016) in both hemispheres over the Sahel and Namibia. Over the Pacific Ocean sector (Fig. 10e), strong upward motion appears over the equator when El Niño events occur. The anomalous convective region, however, tends to stay north of the equator after 1999. Accordingly, the annual mean anomalous precipitation during the recent period exhibits a large increase around 5° N−10° N, but decreases over the equator and the SH (Fig. 10f). Three-monthly mean meridional wind at 925 hPa averaged over the equator (5° S−5° N) and a latitude−time section of 3-monthly anomalous SST of the Niño 3.4 sector are shown in Figs. 10g and 10h, respectively. Before 1999, an increase in equatorial SST was accompanied by a strengthening of convection over the equator and the anomalous southward wind. After 1999, although SST increased over the equator especially during El Niño, the anomalous northward wind was stronger and the convective activity tended to remain in the NH.

3.4 Stratosphere−troposphere connection

The connection between tropospheric and stratospheric circulations around the tropopause region is shown in Figs. 8 and 9. Continuity in a zonally averaged field, however, does not necessarily indicate actual continuity at each location. To confirm continuity within the rising branch of the Hadley circulation from the upper troposphere to the stratosphere, longitude−height sections of the normalized anomalous pressure vertical velocities averaged over 10°−20° latitudes in the summer hemisphere

are displayed in Fig. 11. Horizontal distributions of the anomalous pressure vertical velocity at 150 hPa and the anomalous surface precipitation are also displayed in the lower panels. Anomalous upwelling, extending from the upper troposphere to the lower stratosphere, is connected with the surface precipitation over continents and their vicinity. The vertical structure of the present decadal change in both hemispheres has a similar structure: upwelling tends to be enhanced over the continents, but suppressed over the oceans. Contrast between the continent and ocean sector is clearly seen in the stratosphere of the SH where the distribution of land is simpler. Note also that the variation of surface precipitation is larger over the ocean than over land, but the associated height of the upwelling is lower and has a smaller impact on the stratospheric circulation.

4 Summary and discussion

Characteristics of the recent tropical circulation change from the middle to the end of the 1990s can be summarized as follows. Cooling of the ocean in the equatorial SH occurred in association with a strengthening of cross-equatorial southerlies near the surface, which was induced by a northward shift of the convective zone connected to the rising branch of the Hadley circulation and the stratospheric Brewer−Dobson circulation. The transport of water vapour by the enhanced cross-equatorial southerlies further amplified the convective activity in the NH. An increase in the vertical velocity was most apparent in the TTL. This could be related to a decrease in the static stability in the TTL due to the combined effects of lower stratospheric cooling and upper tropospheric warming. Thus, we conclude that the recent tropical circulation change originates primarily from a strengthening of deep convective activity over the continents and their vicinity in the summer hemisphere, in particular over the African–Asian sector (30° W−150° E). Aumann and Ruzmaikin (2013) reported that deep convection over land in the tropics shows an increasing trend, while that over tropical oceans shows an opposite decreasing trend based on 10 years of Atmospheric Infrared Sounder (AIRS) data.

The impact of the northward shift of summertime Hadley circulation in the Pacific sector is amplified through wind−evaporation−SST (WES) feedback (Fig. 5). During boreal autumn and winter, anomalously active convective centre moves southward to the equatorial Indian Ocean–Maritime Continent region, which induces stronger easterlies over the equatorial central Pacific. As a result, sea surface cooling extends from the equatorial eastern Pacific to the central Pacific. This could explain the recent trend in the suppression of warming in the eastern Pacific including the aborted El Niño of 2014 (Maeda et al., 2016; Wu et al., 2017) and a decrease in the occurrence of east Pacific-type El Niños. It should also be noted that the El Niño of 2015/16 was one of the largest events; however, it was a mixed type with smaller warming in the eastern Pacific (Paek et al., 2017), as can also be seen in the OLR field in Fig. 5.

Results of the present study indicate some similarities between the recent trends in the two summer hemispheres, which can be qualified as a strengthening of the rising branch of the Hadley circulation connected to the stratospheric circulation (Fig. 11). The increasing trend in the Earth's surface temperature is generally attributed to the increase in greenhouse gases like

CO_2 (IPCC, 2013). Such a change in the radiative forcing may explain the global characteristics of the recent change. The effect of increased CO_2 can be divided into a direct radiative effect and an indirect effect through changes in the SST. Model experiments have shown that the direct radiative effect of CO_2 increases tropical upward motion particularly over the Sahelian sector, whereas it suppresses upwelling over the oceanic sector in the Pacific (Fig. 8 of Gaetani et al., 2016). Initial changes in convective activity over land and ocean can be amplified through associated circulation changes: warming of the ocean surface is reduced by increased evaporation, and the water vapour transported to the continents further enhances convective activity over land. In fact, synchrony of the recent increasing trends in Sahelian rainfall with global oceanic evaporation has been documented by Diawara et al. (2016).

The tropospheric response to change in the radiative forcing described above is a fundamental process that should be easily reproduced in global models. However, model simulations using realistic forcings, such as the Coupled Model Intercomparison Project Phase 5 (CMIP5) (Taylor et al., 2012), fail to reproduce the recent cooling tendency in the equatorial Pacific in the model ensemble mean. Therefore the equatorial Pacific cooling is often attributed to the internal variation of the atmosphere–ocean coupled system (Meehl et al., 2014) though it could also be due to model deficiencies. Here we briefly investigate whether the effect of extreme deep penetrating convection on large scale circulation is well simulated in a model. For convenience, we compare the climatological mean vertical velocities from the JRA55 reanalysis and the JRA55-AMIP run. The latter uses the same atmospheric general circulation model and boundary conditions (SST and sea ice) as JRA55, but without the assimilation of observed data (Kobayashi and Iwasaki, 2016). The results show that upwelling in the summer tropics and downwelling in the winter polar stratosphere are weaker in JRA55-AMIP (Fig. 12a). The horizontal distribution of the difference in pressure vertical velocity at 150 hPa (lower panels in Fig. 12a) show that model upwelling is weaker in summer over land and adjacent oceans around 10°–20° in latitude, where deep penetrative convection is frequent (Liu and Zipser, 2005). Regions of weak upwelling in the model coincide with the regions of increasing recent decadal trends in upwelling (see Fig. 9).

The above results based on a general circulation model used for JRA55 reanalysis are common biases found in other models: the NH intertropical convergence zone is weaker and the eastern Pacific SST is warmer compared to observations owing to weaker cross-equatorial winds (Li and Xie, 2014; Richter, 2015). It is also noted that equatorial eastern Pacific SST is very sensitive to the model convective cloud scheme (Braconnot et al., 2007). Because the observed change is the opposite of these model biases, it is possible that the failure of the model to simulate the recent cooling in the tropical eastern Pacific originates from these model deficiencies. The recent decadal trend in the tropical troposphere is connected to the change in the stratosphere, as seen in Figs. 8 and 11. Note that the extreme deep convection penetrating into the TTL is not only influenced by the underlying SST, but is also sensitive to the stratospheric circulation (Wang et al., 2014; Eguchi et al., 2015: Kodera et al., 2015). Therefore, the unsuccessful simulation could be the result of unrealistically low sensitivity to a cooling in the lower stratosphere in the models.

An increase in CO_2 raises the Earth's surface temperature, but also decreases stratospheric temperatures. Such changes in the vertical structure of the atmosphere may create favourable conditions for the development of extreme deep convection penetrating the TTL over and around the continents. At the same time, warming of the upper troposphere over remote oceanic regions where cloud tops are generally lower leads to a suppression of convective activity over the ocean owing to increased static stability. The difference in convective activity over land vs. ocean is further amplified through the transport of water vapour from the ocean to the land. The present working hypothesis (Fig. 13) applies well during boreal summer in particular and where a large land mass is located off the equator. Although an increase in the concentration of CO_2 produces a cooling effect in the stratosphere, recent cooling in the lower stratosphere–tropopause region is largely due to a dynamical effect (Abalos et al., 2015). The sudden decrease in lower stratospheric water vapour around the year 2000 (Randel et al., 2006; Hasebe and Noguchi, 2016) also supports the dynamical forcing of the change. Further investigation is needed to determine whether the stratosphere is merely passively responding to the tropospheric warming or playing an active role in the tropospheric circulation change.

Studies of long-term trends face problems that often arise from changes in the observation systems, stations or the drift of the orbit of the satellites; even reanalysis datasets making use of the same model and the same method of analysis are subject to these artifacts. For instance, a large erroneous decrease in TTL temperatures was found in the NCEP-1 reanalysis around the end of the 1990s (Vecchi et al., 2013), which coincides with the change in the observing system from TOVS to ATOVS at NOAA (Li et al., 2000). Therefore, to avoid these problems and to better understand the stratosphere–troposphere coupling processes, we conducted additional case studies on the northward shift of convective activity similar to that associated with the recent trend, but associated with a sudden cooling of the tropical stratosphere during a boreal summer monsoon (Kodera et al., 2018, paper in preparation). In the present study, we made use of daily mean OLR data to investigate the evolution of convective activity due to its long data record. However, OLR is not the most suitable variable for investigating extreme deep convection that plays a critical role in stratospheric and tropospheric coupling (Kodera et al., 2015). Therefore, a companion paper will investigate the coupling processes by using convective overshooting and cloud top data derived from recent satellite observations.

5 Data availability

Datasets used in this paper are all publicly available. Meteorological reanalysis datasets created by JMA, JRA55, and JRA-AMIP are available from http://search.diasjp.net/en/dataset/JRA55 and http://search.diasjp.net/en/dataset/JRA55_AMIP, respectively. The COBE monthly mean SST dataset can be obtained from the JMA website (http://ds.data.jma.go.jp/tcc/tcc/products/elnino/cobesst/cobe-sst.html). Monthly mean HIRS OLR data can be obtained from

NOAA by FTP (ftp://eclipse.ncdc.noaa.gov/cdr/hirs-olr/monthly/). The GPCP monthly mean precipitation dataset is obtained from the NOAA website (https://www.esrl.noaa.gov/psd/data/gridded/data.gpcp).

Acknowledgements

The authors wish to express their thanks to Beatriz Funatsu, Chantal Claud and Leonhard Pfister for valuable discussions and comments. This work was supported in part by Grants-in-Aid for Scientific Research (25340010, 26281016, and 16H01184) from the Japan Society for Promotion of Science.

References

Abalos, M., Legras, B., Ploeger, F., and Randel, W.J.: Evaluating the advective Brewer-Dobson circulation in three reanalyses for the period 1979–2012, J. Geophys. Res. Atmos.,120, doi:10.1002/2015JD02, 2015.

Adler, R.F., Huffman, G.J., Chang, A., Ferraro, R., Xie, P., Janowiak, J.E., Rudolf, B., Schneider U., Curtis, S., Bolvin. D.T., Gruber, A., Susskind, J., Arkin, P.A., and Nelkin, E.J.: The Version 2 Global Precipitation Climatology Project (GPCP) monthly precipitation analysis (1979-present), J. Hydrometeor, 4, 1147-1167, 2003.

Aumann, H.H. and Ruzmaikin, A.: Frequency of deep convective clouds in the tropical zone from 10 years of AIRS data, Atmos. Chem. Phys., 13, 10795–10806, doi:10.5194/acp-13-10795-2013, 2013.

Braconnot, P., Hourdin, F., Bony, S., Dufresne, J-L., Grandpeix, J-Y., and Marti, O.: Impact of different convective cloud schemes on the simulation of the tropical seasonal cycle in a coupled ocean–atmosphere model, Clim. Dyn., 29, 501–520, doi:10.1007/s00382-007-0244-y, 2007.

Brandt, M., Mbow, C., Diouf, A.A., Verger, A., Samimi, C., and Fensholt, R.: Ground and satellite based evidence of the biophysical mechanisms behind the greening Sahel, Global Change Biol., 21, 1–11, doi:10.1111/gcb.12807, 2014.

Chiang, J C.H., Swenson, L.M., and Kong, W.: Role of seasonal transitions and the westerlies in the interannual variability of the East Asian summer monsoon precipitation, Geophys. Res. Lett., 44, 3788–3795, doi:10.1002/2017GL072739, 2017.

Davis, S.M. and Rosenlof, K.H.: A multidiagnostic intercomparison of tropical-width time series using reanalyses and satellite observations, J. Clim., 25, 1061-1078, 2012.

Diawara, A., Tachibana, Y., Oshima, K., Nishikawa, H., and Ando, Y.: Synchrony of trend shifts in Sahel boreal summer rainfall and global oceanic evaporation 1950–2012, Hydrol. Earth Syst. Sci., 20, 3789–3798, doi:10.5194/hess-20-3789-2016, 2016.

Dong, B. and Dai, A.: The influence of the interdecadal Pacific oscillation on temperature and precipitation over the globe, Climate Dyn, 45(9-10):2667–2681, 2015.

Eguchi, N., Kodera, K., and Nasuno, T.: A global non-hydrostatic model study of a downward coupling through the tropical tropopause layer during a stratospheric sudden warming, Atmos. Chem. Phys., 15, 297–304, 2015.

Emanuel, K., Solomon, S., Folini, D., Davis, S., and Cagnazzo, C.: Influence of tropical tropopause layer cooling on Atlantic hurricane activity, J. Clim., 26, 2288–2301, https://doi.org/10.1175/JCLI-D-12-00242.1, 2013.

England, M.H., McGregor, S., Spence, P., Meehl, G.A., Timmermann, A., Cai, W., Gupta, A.S., McPhaden, M.J., Purich, A., and Santoso, A.: Recent intensification of wind-driven circulation in the Pacific and the ongoing warming hiatus, Nat. Clim.Change, 4, 222–227, doi:10.1038/nclimate2106, 2014.

Evan, A.T. and Camargo, S. J. A: climatology of Arabian Sea cyclonic storms, J. Clim.24, 140–158, 2011.

Fontaine, B., Roucou, P., Gaetani, M., and Marteau, R.: Recent changes in precipitation, ITCZ convection and northern tropical circulation over North Africa (1979–2007), Int. J. Climatol., 31, 633–648, doi:10.1002/joc.2108, 2011.

Gaetani, M., Flamant, C., Bastin, S., Janicot, S., Lavaysse, C., Hourdin, F., Braconnot, P., and Bony, S.: West African monsoon dynamics and precipitation: the competition between global SST warming and CO2 increase in CMIP5 idealized simulations, Clim Dyn., doi:10.1007/s00382-016-3146-z, 2016.

Gautam, D.K. and Regmi, S.K.: Recent trends in the onset and withdrawal of summer monsoon over Nepal, ECOPERSIA, 1(4): 353-367, 2013.

Hagos, S.M. and Cook, K.H.: Dynamics of the West African monsoon jump, J Clim., 20, 5264–5284. doi:10.1175/2007JCLI1533.1, 2007.

Hasebe, F. and Noguchi, T.: A Lagrangian description on the troposphere-to-stratosphere transport changes associated with the stratospheric water drop around the year 2000, Atmos. Chem. Phys., 16, 4235-4249, doi:10.5194/acp-16-4235-2016, 2016.

Hu, S. and Fedorov, A.V.: The extreme El Niño of 2015–2016 and the end of global warming hiatus, Geophys. Res. Lett., 44, doi:10.1002/2017GL072908, 2017.

IPCC: Summary for Policymakers. In: Climate Change 2013: The Physical Science Basis. Contribution of Working Group I to the Fifth Assessment Report of the Intergovernmental Panel on Climate Change, Stocker, T.F., Qin, D., Plattner, G.-K., Tignor, M., Allen, S.K., Boschung, J., Nauels, A., Xia, Y., Bex, V., Midgley, P.M. (eds.), Cambridge University Press, Cambridge, United Kingdom and New York, NY, USA, 2013.

Ishii, M., Shouji, A., Sugimoto, S., and Matsumoto, T.: Objective analyses of sea-surface temperature and marine meteorological variables for the 20th century using ICOADS and the KOBE collection, Int. J. Climatol., 25, 865-879, 2005.

Iwasaki, T. (1992), General circulation diagnosis in the pressure-isentrope hybrid vertical coordinate, J. Meteorol. Soc. Jpn., 70, 673–687, 1992.

Johnson, N.C.: How many ENSO flavors can we distinguish? J. Clim. ,26, 4816–4827, doi:10.1175/JCLI-D-12-00649.1., 2013.

Kajikawa, Y., Yasunari, T., Yoshida, S., and Fujinami, H.: Advanced Asian summer monsoon onset in recent decades, Geophys. Res. Lett., 39, L03803, doi:10.1029/2011GL050540, 2012.

Kamae, Y., X. Li, S.-P. Xie, and Ueda, H.: Atlantic effects on recent decadal trends in global monsoon, Clim. Dyn.., doi:10.1007/s00382-017-3522-3, 2017.

Kang, S. M., and Polvani, L.M.: The interannual relationship between the latitude of the eddy-driven jet and the edge of the Hadley cell, J. Clim., 24, 564–568, 2011.

Kao, H-Y., and Yu, J-Y.: Contrasting eastern‐Pacific and central‐Pacific types of ENSO, J. Clim., 22, 615– 632, doi:10.1175/2008JCLI2309.1., 2009.

Kobayashi, C., and T. Iwasaki: Brewer-Dobson circulation diagnosed from JRA-55, J. Geophys. Res. Atmos., 121, doi:10.1002/2015JD023476, 2016.

Kobayashi, S., Ota, Y., Harada, Y., Ebita, A., Moriya, M., Onoda, H., Onogi, K., Kamahori, H., Kobayashi, C., Endo, H., Miyaoka, K., and Takahashi, K.: The JRA-55 Reanalysis: general specifications and basic characteristics, J. Meteorol. Soc. Japan, 93, 5−48, doi:10.2151/jmsj.2015-001, 2015.

Kodera, K., Funatsu, B.M., Claud, C., and Eguchi, N.: The role of convective overshooting clouds in tropical stratosphere–troposphere dynamical coupling, Atmos. Chem. Phys., 15, 6767-6774, doi:10.5194/acp-15-6767-2015, 2015.

Kodera, K., Ueyama, R., Funatsu, B., Eguchi, N., Pfister, L., and Claud, C.,: Impact of tropical lower stratospheric cooling on deep convective activity: (II) Abrupt seasonal transition in boreal summer monsoon, in preparation, 2018.

Kosaka, Y. and Xie, S.-P.: Recent global-warming hiatus tied to equatorial Pacific surface cooling, Nature, 501, 403–407, doi:https://doi.org/10.1038/nature12534, 2013.

Kuroda, Y., An effective SVD calculation method for climate analysis, J. Meteorol. Soc. Jpn., 76, 647-655, 1998.

Lee, H., Gruber, A., Ellingson, R.G., and Laszlo, I.: Development of the HIRS outgoing longwave radiation climate dataset. J. Atmos. Oceanic Technol., 24, 2029–2047, doi: 10.1175/2007JTECHA989.1, 2007.

Li, G. and Xie, S.-P.: Tropical biases in CMIP5 multimodel ensemble: The excessive equatorial Pacific cold tongue and double ITCZ problems, J. Clim., 27, 1765–1780, doi: 10.1175/JCLI-D-13-00337.1, 2014.

Li, J., Wolf, W.W., Menzel, W.P., Zhang, W., Huang, H., and Achtor, T.H.: Global soundings of the atmosphere from ATOVS measurements: The algorithm and validation, J. Appl. Meteor., 39, 1248–1268, doi.org/10.1175/1520-0450(2000)039<1248:GSOTAF>2.0.CO;2, 2000.

Liu, B. and Zhou, T., Atmospheric footprint of the recent warming slowdown, Scientific Reports, 7, 40947, doi:10.1038/srep40947, 2017.

Liu, C. and Zipser, E.J.: Global distribution of convection penetrating the tropical tropopause, J. Geophys. Res., 110, D23104, doi:10.1029/2005JD006063, 2005.

Maeda, S., Urabe, Y., Takemura, K,. Yasuda, T., and Tanimoto, Y.: Active role of the ITCZ and WES feedback in hampering the growth of the expected full-fledged El Niño in 2014, SOLA, 12, 17−21, doi:10.2151/sola.2016-004, 2016.

Maidment, R.I., Allan, R.P., and Black, E.: Recent observed and simulated changes in precipitation over Africa, Geophys. Res. Lett., 42, 8155–8164, doi:10.1002/2015GL065765, 2015.

Meehl, G.A., Hu, A., Arblaster, J.M., Fasullo, J., and Trenberth, K.E.: Externally forced and internally generated decadal climate variability associated with the interdecadal Pacific oscillation, J. Clim., 26, 7298–7310, doi:10.1175/JCLI-D-12-00548.1., 2013.

Meehl, G.A., Teng, H., Arblaster, J.M.: Climate model simulations of the observed early-2000s hiatus of global warming, Nat. Clim. Change, doi:10.1038/nclimate, 2014.

Paek, H., Yu, J.-Y., and Qian, C.: Why were the 2015/2016 and 1997/1998 extreme El Niños different? Geophys. Res. Lett., 44, doi:10.1002/2016GL071515, 2017.

Ramsay, H.: The effects of imposed stratospheric cooling on the maximum intensity of tropical cyclones in axisymmetric radiative–convective equilibrium, J. Clim., 26, 9977–9985, doi: 10.1175/JCLI-D-13-00195.1., 2013.

Randel, W.J. and Jensen, E.J. : Physical processes in the tropical tropopause layer and their roles in a changing climate, Nat. Geosci., 6, 169–176, doi:10.1038/ngeo1733, 2013.

Randel, W.J., Wu, F., Vömel, H., Nedoluha, G.E., and Forster, P.: Decreases in stratospheric water vapor after 2001: links to changes in the tropical tropopause and the Brewer–Dobson circulation, J. Geophys. Res., 111, D12312, doi:10.1029/2005JD006744, 2006.

Richter,I.: Climate model biases in the eastern tropical oceans: causes, impacts and ways forward, WIREs Clim Change, doi: 10.1002/wcc.338, 2015.

Taylor, K.E., Ronald, J.S., and Meehl, G.A.: An overview of CMIP5 and the experiment design, Bull. Amer. Meteor. Soc., 93, 485–498, 2012.

Trenberth, K. E.: Has there been a hiatus? Science, 349(6249), 691–692, 2015.

Trenberth, K. E., Fasullo, J.T., Branstator, G. and, Phillips, A.: Seasonal aspects of the recent pause in surface warming, Nat. Clim. Change, doi:10.1038/nclimate2341, 2014.

Urabe, Y., Yasuda, T., and Maeda, S.: Rapid warming in global sea surface temperature since around 2013, SOLA, 13, 25−30, doi:10.2151/sola.2017-005., 2017.

Vecchi, G.A., Fueglistaler, S., Held, I.M., Knutson, T.R., and Zhao, M.: Impacts of atmospheric temperature trends on tropical cyclone activity, J. Clim., 26, 3877–3891, https://doi.org/10.1175/JCLI-D-12-00503.1, 2013.

Vizy, E.K., and Cook, K.H.: Understanding long-term (1982–2013) multi-decadal change in the equatorial and subtropical South Atlantic climate, Clim. Dyn., 46: 2087, doi:10.1007/s00382-015-2691-1, 2016.

Wang, B., Xu, S., and Wu, L.: Intensified Arabian Sea tropical storms, Nature 489, E1–E2, doi:10.1038/nature11470, 2012.

Wang, B., Liu, J., Kim, H-J,, Webster, P.J., Yim, S-Y., and Xiang, B.: Northern Hemisphere summer monsoon intensified by mega-El Niño/southern oscillation and Atlantic multidecadal oscillation, Proc Natl Acad Sci U S A, 110, 5347–5352, 2013.

Wang, S., Camargo, S.J., Sobel, A.H., and Polvani, LM.: Impact of the tropopause temperature on the intensity of tropical cyclones—an idealized study using a mesoscale mode, J. Atmos. Sci., 71, 4333–4348, 2014.

Watanabe, M., Shiogama, H., Tabete, H., Hayashi, M., Ishii, M., and Kimoto, M.: Contribution of natural decadal variability to global warming acceleration and hiatus, Nat. Clim. Change, doi:10.1038/nclimate2355, 2014.

Wu, Y.-K., L. Chen, Hong, C.-C., Li, T., Chen, C.-T., and Wang, L.: Role of the meridional dipole of SSTA and associated cross-equatorial flow in the tropical eastern Pacific in terminating the 2014 El Niño development, Clim. Dyn., 2017.

Xiang, B. and Wang, B.: Mechanisms for the advanced Asian summer monsoon onset since the mid-to-late 1990s, J. Clim., 26, 1993–2009, 2013.

Xie, S.-P.: The shape of continents, air-sea interaction, and the rising branch of the Hadley circulation, in The Hadley Circulation, Past, Present and Future, edited by: Diaz, H. F. and Bradley, R. S., Kluwer Academic Publishers, Dordrecht, the Netherlands, 121–152, 2004.

Xie, S.-P. and Kosaka, Y.: What caused the global surface warming hiatus of 1998–2013? Curr. Clim. Change Rep., doi:10.1007/s40641-017-0063-0, 2017.

Xie, S.-P. and Philander, S.G.H.: A coupled ocean-atmosphere model of relevance to the ITCZ in the eastern Pacific, Tellus, 46A, 340−350, 1994.

Yun, K.-S., Lee, J.-Y., and Ha, K.-J.: Recent intensification of the South and East Asian monsoon contrast associated with an increase in the zonal tropical SST gradient, J. Geophys. Res. Atmos., 119, 8104–8116, doi:10.1002/2014JD021692, 2014.

Atmos. Chem. Phys. Discuss., https://doi.org/10.5194/acp-2018-128
Manuscript under review for journal Atmos. Chem. Phys.
Discussion started: 16 February 2018

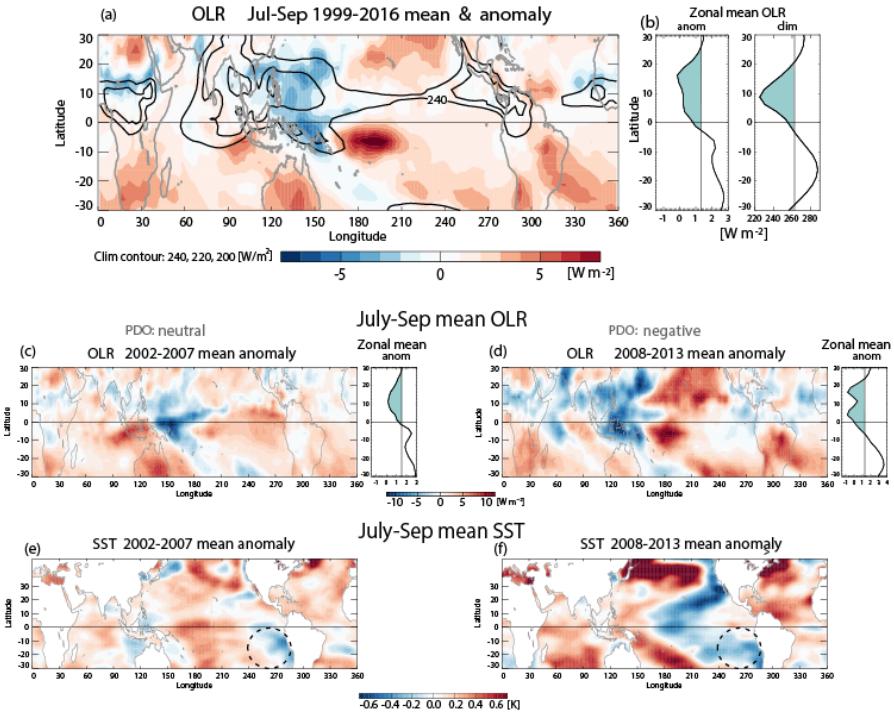

Figure 1: (a) Climatological (1981-2010) July–September mean OLR (contours: 240, 220, and 200 W m^{-2}) and anomalous July–September OLR (departures from climatology) in 1999-2016 (color shading). (b) Zonal mean profiles of (a): anomalies from climatology (left) and climatology (right). (c) Anomalous OLR as in (a) and (b, left) but for 2002-2007 period. (d) Anomalous OLR as in (a) and (b, left) but for 2008-2013 period. (e,f) Anomalous July–September SST (departures from climatology) in 2002-2007 (e) and 2008-2013 (f).

Atmos. Chem. Phys. Discuss., https://doi.org/10.5194/acp-2018-128
Manuscript under review for journal Atmos. Chem. Phys.
Discussion started: 16 February 2018

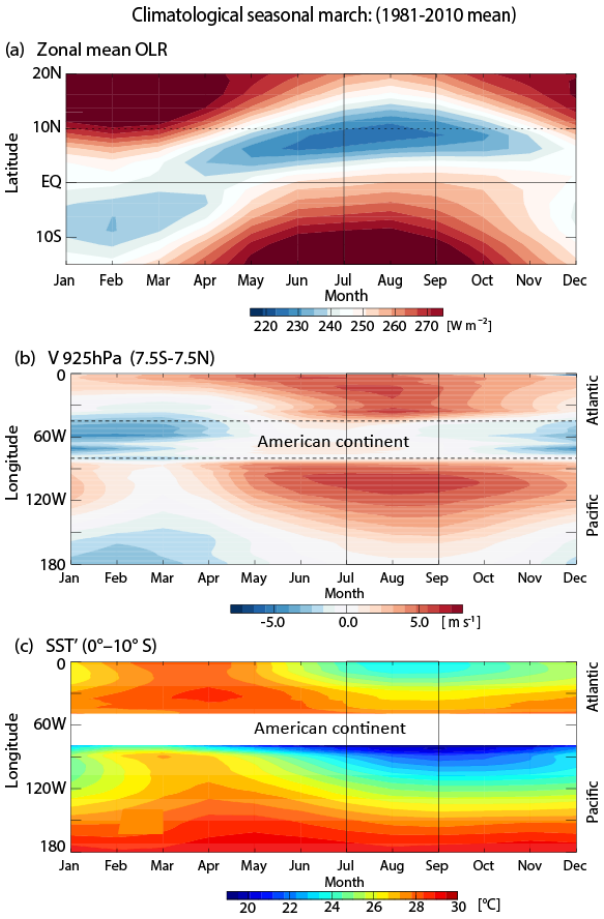

Figure 2: Climatological (1981-2010) annual cycle. (a) Latitude–time section of zonal mean OLR. (b) Longitude–time section of the equatorial mean (7.5° S–7.5° N) meridional wind component at 925 hPa over the eastern Pacific–Atlantic sector. (c) Longitude–time section of southern equatorial (0°–10° S) SSTs over the eastern Pacific–Atlantic sector.

Atmos. Chem. Phys. Discuss., https://doi.org/10.5194/acp-2018-128
Manuscript under review for journal Atmos. Chem. Phys.
Discussion started: 16 February 2018

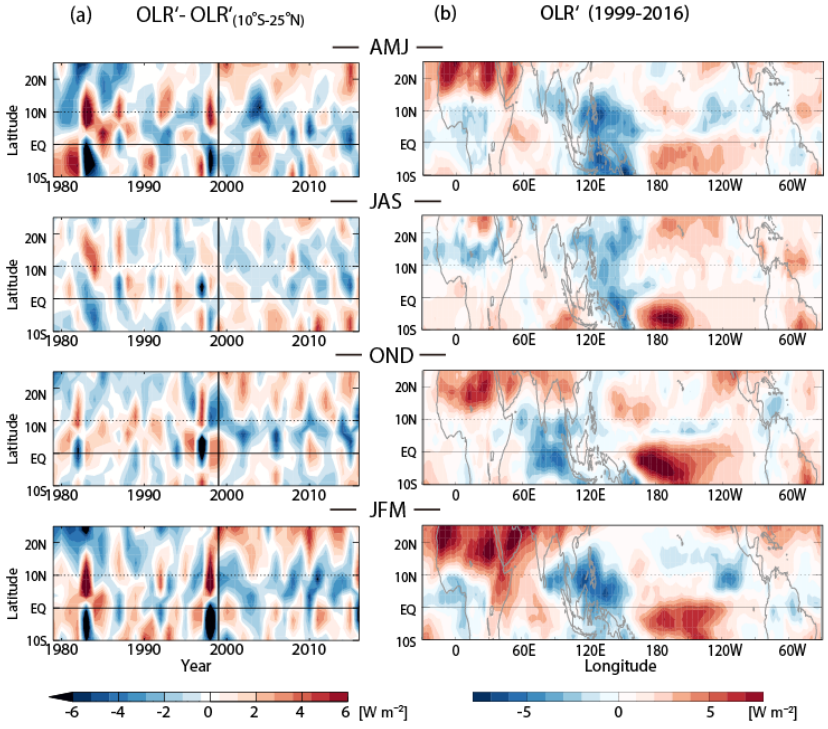

Figure 3: (a) Latitude–time sections of 3-month seasonal mean, zonally-averaged anomalous (departures from 1981-2010 climatological tropical 10° S–25° N mean) OLR in 1979-2016. Vertical solid lines indicate the year 1999. (b) Horizontal distributions of 3-month seasonal mean anomalous OLR from climatology during 1999/2000–2015/2016 period.

Atmos. Chem. Phys. Discuss., https://doi.org/10.5194/acp-2018-128
Manuscript under review for journal Atmos. Chem. Phys.
Discussion started: 16 February 2018

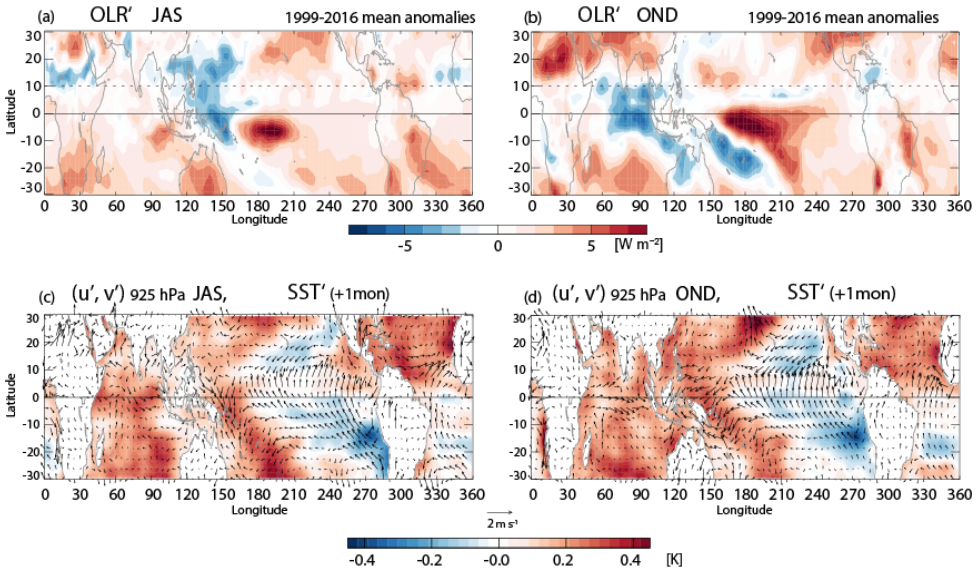

Figure 4: (a) JAS and (b) OND mean anomalous OLR for the period 1999-2016. (c) JAS and (d) OND mean anomalous horizontal winds at 925 hPa (arrows) for the period 1999–2016 superimposed on anomalous SSTs (color shading) with a one-month lag (i.e., ASO and NDJ, respectively).

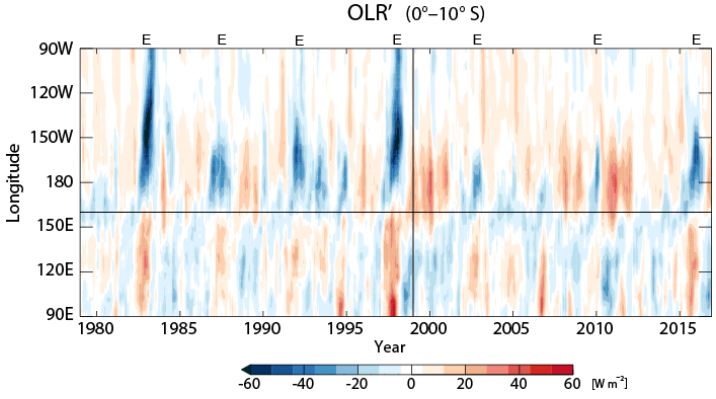

Figure 5: Longitude–time section over the Indian and Pacific Oceans (90° E–90° W) sector of anomalous 3-monthly mean OLR (departures from climatology) averaged over the equatorial SH (0°–10° S). "E" denotes an El Niño event.

Atmos. Chem. Phys. Discuss., https://doi.org/10.5194/acp-2018-128
Manuscript under review for journal Atmos. Chem. Phys.
Discussion started: 16 February 2018

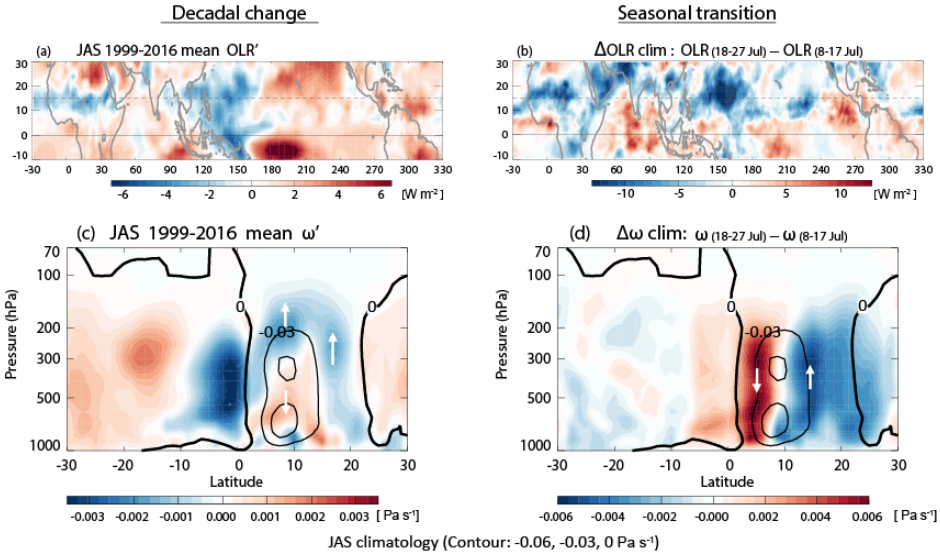

Figure 6: Comparison between (left) recent (1999-2016) decadal anomalies and (right) the climatological mean seasonal transition around 18 July. (a) Anomalous OLR in JAS 1999-2016 (departures from 1981-2010 climatology). (b) Difference between climatological 10-day mean OLR in 18–27 July and 8–17 July. (c) Meridional section of anomalous zonal mean pressure velocity (color shading) in JAS 1999–2016 (departures from 1981-2010 climatology). (d) Meridional section of the difference between climatological 10-day mean, zonal mean pressure vertical velocity (color shading) in 18–27 July and 8–17 July. Climatological JAS mean, zonal mean pressure velocity is indicated as contours (0, –0.03, and –0.06 Pa s^{-1}) in (c) and (d). Arrows indicate upward and downward anomalous winds.

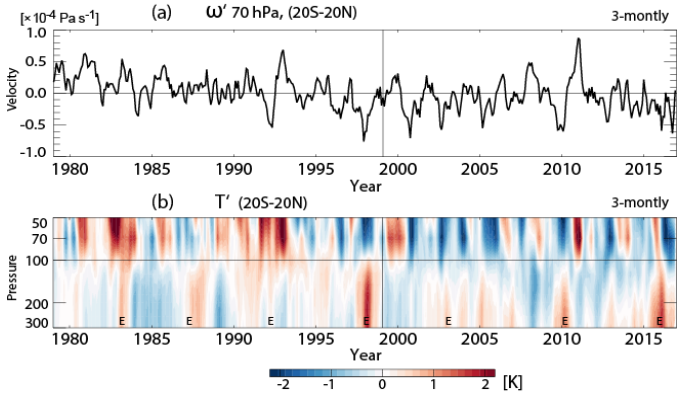

Figure 7: (a) 3-month mean anomalous pressure vertical velocity in the tropics (20° S–20° N) at 70 hPa. (b) Height–time section of 3-month mean anomalous temperature in the tropics (20° S–20° N). "E" denotes an El Niño event.

Atmos. Chem. Phys. Discuss., https://doi.org/10.5194/acp-2018-128
Manuscript under review for journal Atmos. Chem. Phys.
Discussion started: 16 February 2018

Atmospheric Chemistry and Physics
Discussions

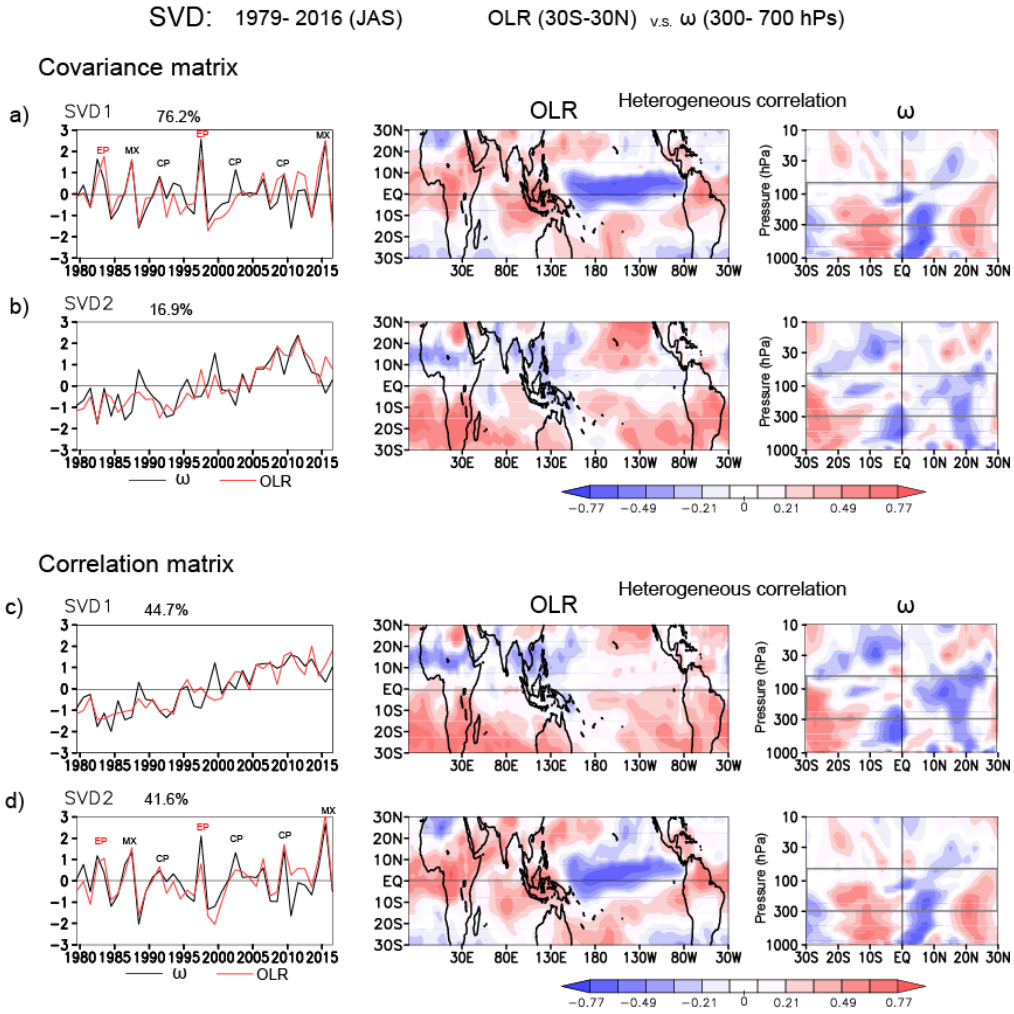

Figure 8: SVD analysis of the zonal mean anomalous pressure velocity in the upper troposphere–lower stratosphere (300–70 hPa: gray lines) and anomalous OLR (0°–360° E) in the tropics (30° S–30° N) during JAS from 1979 to 2016. (a) Leading mode and (b) second mode based on the covariance matrix: (from left to right) time coefficients, heterogeneous correlation of OLRs, and heterogeneous correlation map of the pressure velocity extended to 1000–10 hPa. Percentage of explained covariance by the respective modes are indicated above the time coefficients. (c,d) As in (a) and (b), respectively, but for the SVD based on the correlation matrix. "EP", "CP", and "MX" indicate different types of El Niño events (Peak et al., 2017): EP, eastern Pacific; CP, central Pacific; MX, mixed type.

Atmos. Chem. Phys. Discuss., https://doi.org/10.5194/acp-2018-128
Manuscript under review for journal Atmos. Chem. Phys.
Discussion started: 16 February 2018

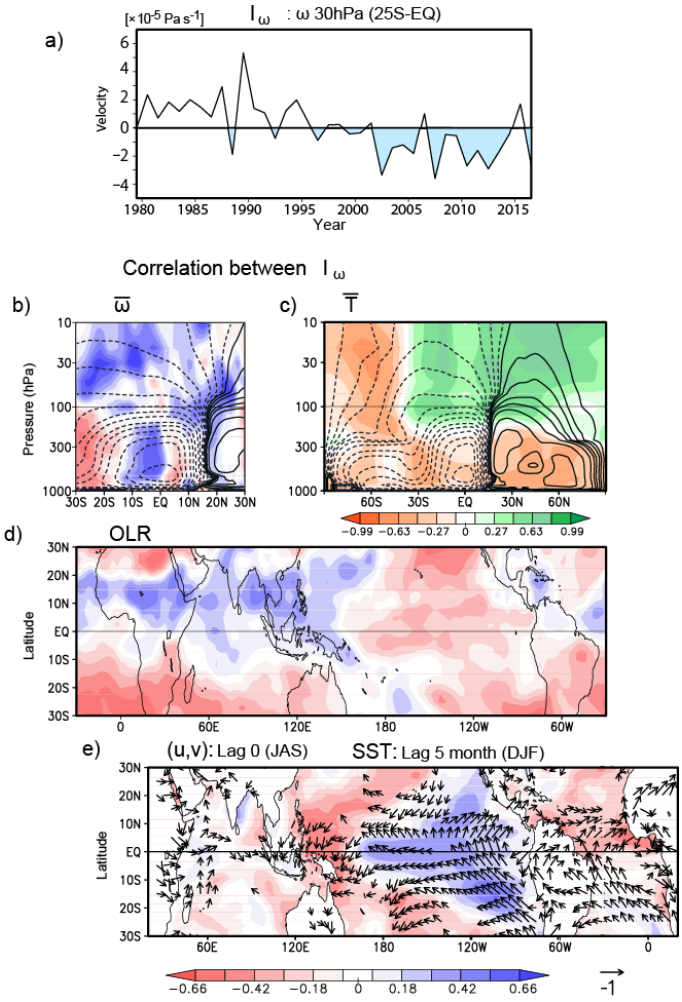

Figure 9: (a) Time series of JAS mean vertical pressure velocity (ω) at 30 hPa averaged over 0°–25° S as an index for the tropical stratospheric vertical velocity (I_ω). Correlation coefficients between I_ω and (b) zonal mean ω, (c) zonal mean temperature T at each grid, (d) OLR, and (e) horizontal winds at 925 hPa (arrows). Lagged correlation with DJF mean SST is also presented as colored shading in (e). Contours in (b) and (c) indicate the climatological residual mean meridional circulation in JAS. Solid and dashed lines indicate clockwise and counterclockwise directions, respectively.

Atmos. Chem. Phys. Discuss., https://doi.org/10.5194/acp-2018-128
Manuscript under review for journal Atmos. Chem. Phys.
Discussion started: 16 February 2018

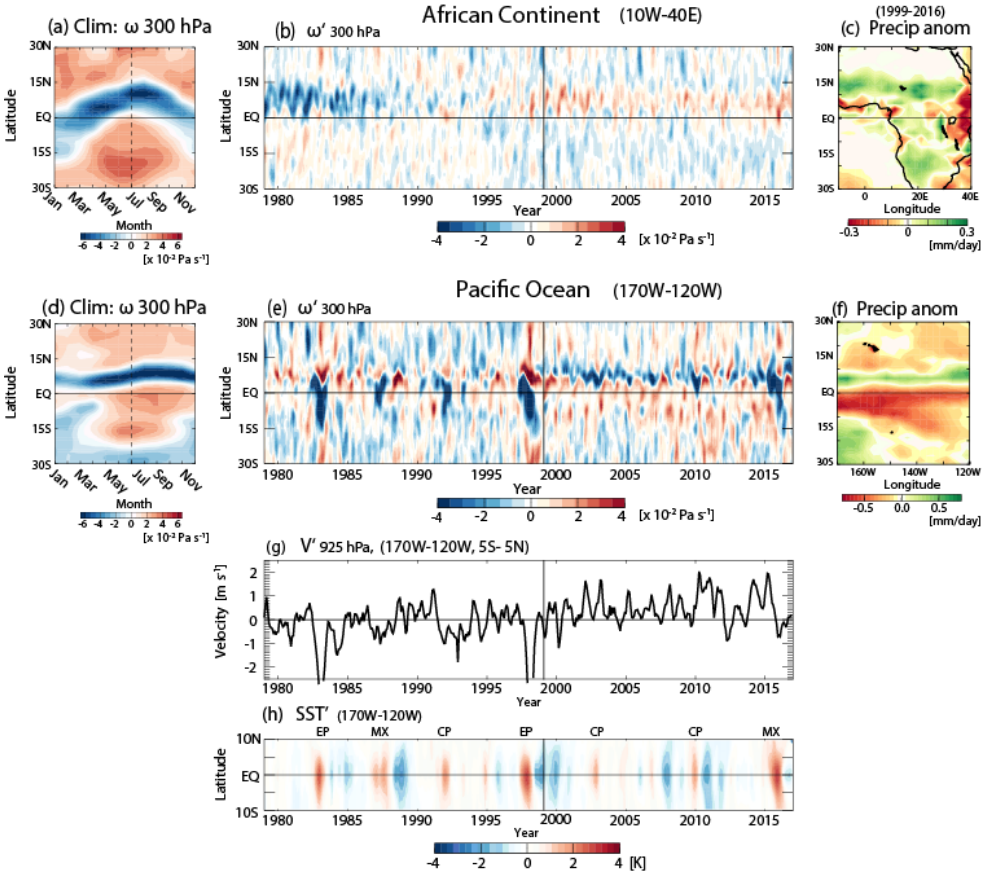

Figure 10: (a) Latitude–time section of the climatological zonal-mean pressure vertical velocity at 300 hPa averaged over the African sector (10° W–40° E). (b) Latitude–time section of monthly mean anomalous pressure vertical velocity from February 1979 to November 2016. (c) Latitude–longitude map of annual mean anomalous precipitation during 1999–2016 over the African sector. (d–f) As in (a–c) but for the eastern Pacific, Niño 3.4 (170° W–120° W) sector. (g) Monthly mean anomalous meridional wind around the Equator (5° S–5° N) over the Niño 3.4 sector. (h) Monthly mean anomalous SST over the Nino 3.4 sector. "EP", "CP", and "MX" indicate different types of El Niño events (Peak et al., 2017): EP, eastern Pacific; CP, central Pacific; MX, mixed type. (b, e, g, h) Three monthly running mean has been applied on data prior to the presentation.

Atmos. Chem. Phys. Discuss., https://doi.org/10.5194/acp-2018-128
Manuscript under review for journal Atmos. Chem. Phys.
Discussion started: 16 February 2018

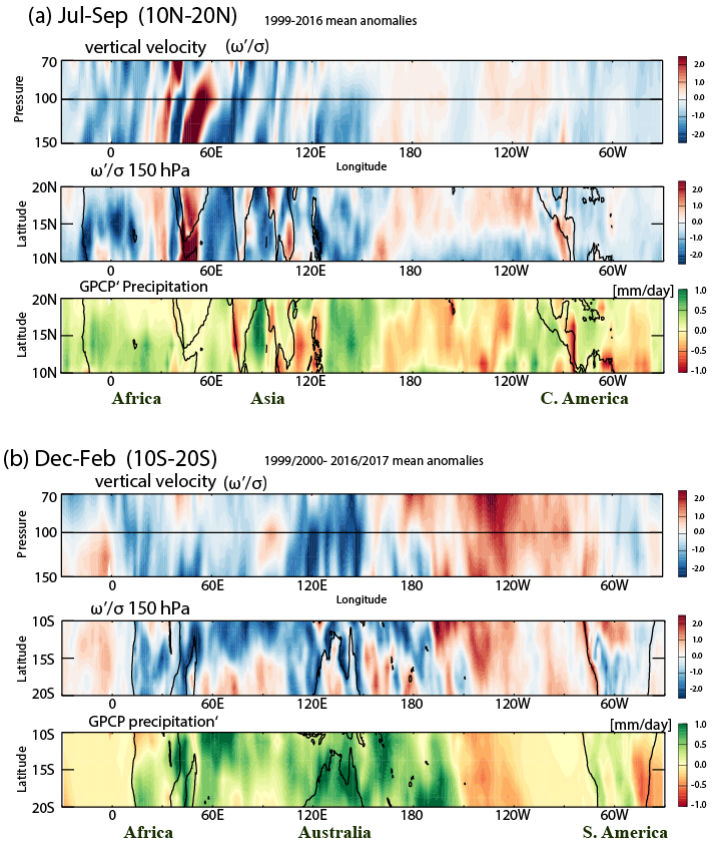

Figure 11: (a) (top panel) Height–longitude section of the standardized (with respect to the interannual variation) anomalous pressure vertical velocity averaged over 10° N–20° N, during boreal summer (JAS) 1999–2016. (middle panel) Standardized pressure vertical velocity at 150 hPa during boreal summer (JAS) 1999–2016. (bottom panel) As in the middle panel, but for surface precipitation. (b) As in (a), but for 10° S–20° S in austral summer (DJF).

Atmos. Chem. Phys. Discuss., https://doi.org/10.5194/acp-2018-128
Manuscript under review for journal Atmos. Chem. Phys.
Discussion started: 16 February 2018

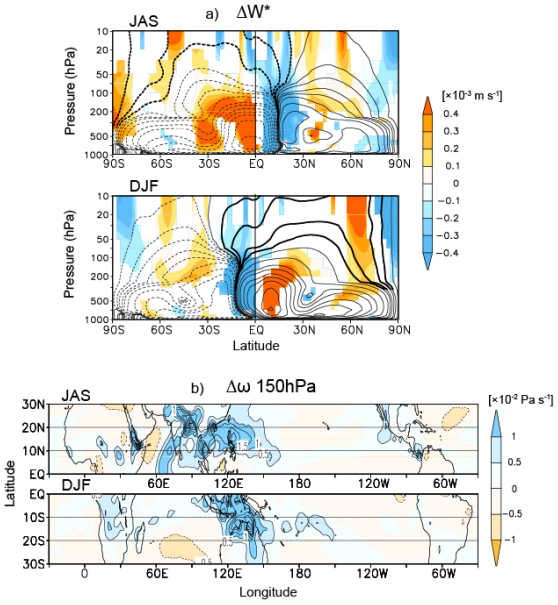

Figure 12: (a) Difference in the climatological JAS (top) and DJF (bottom) mean residual vertical velocity between JRA55-AMIP and JRA55 reanalyses (color shading). Contours indicate the mass stream function of the mean residual circulation in JRA55-AMIP. Streamlines connected to the winter polar stratosphere from the tropics are highlighted using thick lines. Solid and dashed lines represent clockwise and counterclockwise circulations, respectively. Statistically significant differences are indicated in color. (b) Difference in pressure vertical velocity at 150 hPa between JRA55-AMIP and JRA55 reanalyses in the summer tropics: (top) JAS in the NH and (bottom) DJF in the SH.

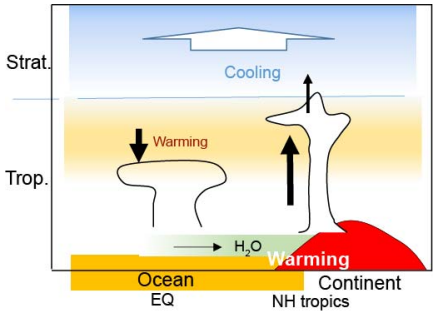

Figure 13: Schematic of the recent changes in the tropics from the late 1990s. Earth's surface warms while the tropical stratosphere cools in response to enhanced stratospheric upwelling. This tends to enhance extreme deep convective activity penetrating the TTL in boreal summer over land, but reduces deep convective activity over equatorial oceans. Differences in convective activity are further amplified through the transport of water vapour in the lower troposphere. (See text for details.)